Enhanced Cross Polarization in Magic Angle Spinning NMR of Metal Complexes†

May Han,‡ Olve B. Peersen,‡ James W. Bryson,§ Thomas V. O'Halloran,§ and Steven O. Smith*,‡

Department of Molecular Biophysics and Biochemistry, Yale University, New Haven, Connecticut 06520, and Department of Chemistry, Northwestern University, Evanston, Illinois 60208

Received June 22, 1994⊗

Solid-state NMR measurements of $S = {}^1/_2$ metal nuclei, such as ^{113}Cd and ^{199}Hg, report directly on the nature and coordination geometry of the ligands in metal complexes. The combination of cross polarization (CP) and magic angle spinning (MAS) has been the standard approach for obtaining high-resolution NMR spectra of these compounds in the solid state. High-speed MAS is usually desirable in order to average the extremely large chemical shift anisotropy of metal nuclei and increase signal intensity. However, the interference of MAS with the CP efficiency at high speeds normally results in weak signals as well as an increased dependence on the exact Hartmann−Hahn matching condition. As a result, it is difficult in practice to locate and maintain an optimal CP match. In this paper, we describe the successful application of variable-amplitude cross polarization (VACP: Peersen et al. *J. Magn. Reson., Ser. A.* **1993**, *104*, 334−339) to CP-MAS NMR studies of two metal complexes, $[Me_4N]_2[Cd_2(S^iPr)_6]$ and $[Me_4N][Hg(S^iPr)_3]$. In VACP, the strength of the spin-lock field is varied to generate multiple matching conditions in a single CP contact period, giving rise to high signal intensity that is independent of the exact Hartmann−Hahn match. VACP can also increase the signal intensity by compensating for the effect of B_1 field inhomogeneity across the sample coil. The results presented in this paper illustrate how VACP can greatly facilitate data acquisition of metal complexes at high MAS speeds and can generally be applied with improved performance to those systems where conventional CP is effective.

Introduction

The development of spectroscopic methods which are sensitive to the coordination environment of transition metal complexes is of considerable importance in the fields of inorganic chemistry and biochemistry. NMR spectroscopy of $S = {}^1/_2$ nuclei, especially ^{113}Cd, has been used extensively in the past decade to characterize metal complexes[1] and has served as a probe for the structure of protein sites that originally bind to spectroscopically silent nuclei, such as Ca^{2+} or Zn^{2+}.[2] It is becoming apparent that NMR measurements on other $S = {}^1/_2$ nuclei, for example ^{199}Hg, will be useful for reporting directly on the metal coordination environment of Hg(II) receptors such as MerR,[3] mercury resistance proteins and Hg-substituted metalloproteins.[4] Spectroscopic characterizations of model compounds with known structure are key to correlating chemical shift data with the nature and geometry of the metal ligands. Solid-state NMR spectroscopy is particularly advantageous in such studies and provides more information than can be obtained from solution NMR measurements of isotropic chemical shifts alone. Detailed analysis of the chemical shift tensor for compounds of known structure can reveal information about the coordination geometry in both crystalline and noncrystalline samples. Furthermore, complications arising from dynamic exchange, low solubility, and slow rotational correlation times of large proteins in solution can be avoided in the solid state. In this article, we describe the application of variable-amplitude cross polarization for increasing the sensitivity of solid-state NMR measurements of metal model complexes. This approach promises to be of practical importance for solid-state NMR studies of metalloproteins which have been hindered by the low sensitivity characteristic of highly anisotropic metal coordination sites.

Proton cross polarization (CP) combined with magic angle spinning (MAS) has been the standard approach used in solid-state NMR studies of ^{113}Cd and ^{199}Hg complexes.[1-3,5] CP produces a substantial increase in sensitivity as compared to the single-pulse Bloch decay experiment primarily for two reasons. First, the high proton gyromagnetic ratio (γ_H) leads to a large magnetization in the proton spins (H) that can be transferred to the metal nuclei (X) by simultaneous CP pulses. These pulses produce B_1 fields whose amplitudes are adjusted experimentally to satisfy the Hartmann−Hahn matching condition, $\gamma_H B_{1H} = \gamma_X B_{1X}$. This results in equal precession frequencies ($\omega_{1H} = \omega_{1X} = \gamma B_1$) around the induced B_1 fields and allows magnetization transfer to occur from the proton spins to the metal nuclei. The maximum theoretical increase in the signal intensity is equal to the γ_H/γ_X ratio. Second, CP permits a shorter recycle time and more rapid data acquisition, because the recycle time is determined by the *proton* T_1 which is invariably shorter than that of the metal nuclei in solids. Magic

* To whom correspondence should be addressed.

† This work was supported by a grant from the National Institutes of Health to S.O.S. (GM-41412).

‡ Yale University.

§ Northwestern University.

⊗ Abstract published in *Advance ACS Abstracts,* January 15, 1995.

(1) Harris, R. K.; Sebald, A. *Magn. Reson. Chem.* **1987**, *25*, 1058−1062.

(2) (a) Armitage, I. M.; Boulanger, Y. In *NMR of Newly Accessible Nuclei;* Laszlo, P., Ed.; Academic Press: New York, 1983; pp 337−365. (b) Ellis, P. D. *Science* **1983**, *221*, 1411−1416. (c) Summers, M. F. *Coord. Chem. Rev.* **1988**, *86*, 43−134. (d) Rivera, E.; Kennedy, M. A.; Ellis, P. D. *Adv. Magn. Reson.* **1989**, *13*, 257−273. (e) Armitage, I. M.; Uiterkamp, A. J. M. S.; Chlebowski, J. F.; Coleman, J. E. *J. Magn. Reson.* **1978**, *29*, 375−392.

(3) Wright, J. G.; Natan, M. J.; MacDonnell, F. M.; Ralston, D. M.; O'Halloran, T. V. *Prog. Inorg. Chem.* **1990**, *38*, 323−412.

(4) Utschig, L.; Wright, J. G.; O'Halloran, T. V. *Methods Enzymol.* **1993**, *226*, 71−97.

(5) (a) Natan, M. J.; Millikan, C. F.; Wright, J. G.; O'Halloran, T. V. *J. Am. Chem. Soc.* **1990**, *112*, 3255−3257. (b) Santos, R. A.; Gruff, E. S.; Koch, S. A.; Harbison, G. S. *J. Am. Chem. Soc.* **1991**, *113*, 469−475.

0020-1669/95/1334-1187$09.00/0

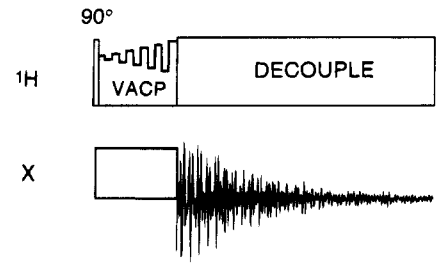

Figure 1. Variable-amplitude cross polarization (VACP) pulse sequence illustrating the application of eleven proton amplitudes. The proton 90° pulse length was set at 4 $\mu\sigma$ (62.5 kHz). The first amplitude corresponds to a 47 kHz ω_{1H} spin-lock frequency and is followed by amplitudes increased or decreased in 1.3 kHz steps in the order illustrated.

angle spinning also increases sensitivity in the CP-MAS experiment by averaging the chemical shift anisotropy (CSA) into a centerband resonance at the isotropic chemical shift and sets of rotational sidebands spaced by the MAS frequency (ω_R). Metal nuclei usually have extraordinarily large CSAs, up to 3000 ppm, which arise from the highly nonsymmetrical distribution of electrons surrounding the nucleus. High-speed MAS is therefore advantageous for these systems because it can potentially increase the signal-to-noise ratio by reducing the number of the rotational sidebands and concentrating the signal intensity into the centerband and remaining sidebands.

Unfortunately, the combination of proton CP and high-speed MAS has a major drawback that severely hinders the study of metal complexes. Under high-speed MAS, the intensity gained by CP is often lost because the CP efficiency is lower and it is more difficult to establish and maintain the exact Hartmann–Hahn match. These effects drastically reduce the intensity of the resulting spectrum. The CP efficiency at different matching conditions can be presented as a plot of signal intensity versus $\Delta\omega_1$, the difference in the H and X spin-lock frequencies, $\Delta\omega_1 = \omega_{1X} - \omega_{1H}$. Such a plot is referred to as the Hartmann–Hahn matching profile. At low MAS speeds, the profile exhibits a broad plateau due to strong proton dipolar couplings and the maximum signal is insensitive to the matching condition. However, when ω_R is comparable to the H–X heteronuclear dipolar couplings, the matching profiles are modulated by ω_R and are broken up into a series of sharp peaks with maximum signal at $\Delta\omega_1 = n\omega_R$, where $n = 0, \pm1, \pm2$, etc.[6] This oscillation results in a situation where a small shift of a few kilohertz from the exact matching condition can lead to a complete loss of signal. For systems that have low sensitivity, such as metal nuclei in proteins, high-speed CP-MAS experiments become nearly impossible because of the formidable task of locating an optimal match and then maintaining it over long experimental times. Furthermore, in metal complexes, the oscillation sets in at relatively low ω_R because the heteronuclear dipolar interactions are usually weak due to the lack of covalent metal–proton bonds. As a result, the large increases in the signal-to-noise ratio expected from high-speed MAS through averaging of the CSA are not realized at these spinning speeds.

Recently, variable-amplitude cross polarization (VACP) has been developed to facilitate data acquisition at high MAS speeds.[7] Rather than using a constant spin-lock field as in conventional or single-amplitude cross polarization (SACP), the VACP experiment incorporates a series of CP pulses on the proton channel with different amplitudes (Figure 1). The amplitudes can be implemented either in an up/down arrangement as in Figure 1 or as a linear ramp.[8] This generates multiple matching conditions within a single acquisition and can remove the oscillations in the Hartmann–Hahn profiles of ^{13}C nuclei spinning at MAS frequencies as high as 15 kHz.[7] VACP can also significantly increase the sensitivity by compensating for the signal losses due to the effect of B_1 field inhomogeneity across the sample.[9] In this paper, we present the application of VACP-MAS to the study of two metal complexes, $[Me_4N]_2[Cd_2(S^iPr)_6]$ and $[Me_4N][Hg(S^iPr)_3]$. These model compounds have large chemical shift anisotropies and weak proton–metal dipolar couplings, representative of the situation in many organometallic complexes and metalloproteins. We compare VACP and SACP at several MAS frequencies and demonstrate that VACP greatly improves the sensitivity of the CP-MAS experiment on these systems. VACP can be used in a general fashion for those systems where CP can be applied. Several experimental parameters that must be considered to optimize data acquisition using VACP are also discussed.

Methods and Materials

Mercuric oxide, cadmium oxide, 2-propanethiol, tetramethylammonium hydroxide solutions (Aldrich, Milwaukee, WI), and all solvents, which were of the highest purity obtainable, were used as supplied. Preparations were carried out under an atmosphere of dry prepurified N_2 (Air Products, Allentown, PA), although final products were handled in air and stored in desiccators. Melting point data were obtained using a Büchi 510 oil bath melting point apparatus. Elemental analyses were carried out by the J. D. Searle Co., Skokie, IL.

$[Me_4N][Hg(S^iPr)_3]$. The method of Bowmaker et al.[10] was adapted as described by Watton.[11] HgO (2.2 g, 10 mmol) was added to a solution of 2-propanethiol (5.6 mL, 4.59 g, 60 mmol) and Me_4NOH (14.6 mL, 25% in MeOH, 3.65 g, 40 mmol) in 25 mL of EtOH. The HgO dissolved within 30 min with stirring under N_2, and the resulting solution was concentrated *in vacuo* with heating to 45 °C until a precipitate was formed. The precipitate redissolved upon heating to 50 °C, and the solution was allowed to cool slowly to room temperature and then placed at −4 °C overnight. The colorless crystals were collected by vacuum filtration, washed with cold EtOH and then diethyl ether, and dried *in vacuo* to give a yield of 2.1 g (42%); mp = 158.5–159.0 °C. Anal. Calcd for $C_{13}H_{33}NS_3Hg$: C, 31.22; H, 6.65; N, 2.80. Found: C, 30.68; H, 6.68; N, 3.02.[11,12]

$[Me_4N]_2[Cd_2(S^iPr)_6]$. Similarly, CdO (1.28 g, 10 mmol) was added to a stirred solution of 2-propanethiol (5.6 mL, 60 mmol) and tetramethylammonium hydroxide (14.6 mL, 25% in methanol, 35 mmol) under N_2, and the mixture was stirred until the CdO dissolved (ca. 20 min). The resultant clear yellow solution was concentrated *in vacuo* with heating to 50 °C, and the solution was allowed to cool slowly. Clear colorless crystals were collected by filtration, washed with cold ethanol, and dried *in vacuo*. Yield = 1.87 g (45%); mp > 260 °C. Anal. Calcd for $C_{26}H_{66}N_2Cd_2S_6$: C, 37.90; H, 8.07; N, 3.40. Found: C, 37.76; H, 8.05; N, 3.42.[13]

CP-MAS spectra were obtained using a multinuclear 5 mm high-speed MAS probe (Doty Scientific, Columbia, SC) on a Chemagnetics 360 MHz solid state spectrometer capable of amplitude modulation of the rf power. The carrier frequencies for the ^{199}Hg and ^{113}Cd experiments were 64.38 and 79.77 MHz, respectively. The pulse programmer of the CMX spectrometer allows control of the B_1 field

(6) Stejskal, E. O.; Schaefer, J.; Waugh, J. S. *J. Magn. Reson.* **1977**, *28*, 105–112.
(7) Peersen, O. B.; Wu, X.; Kustanovich, I.; Smith, S. O. *J. Magn. Reson., Ser. A* **1993**, *104*, 334–339.
(8) Metz, G.; Wu, X.; Smith, S. O. *J. Magn. Reson., Ser. A* **1994**, *110*, 219–227.
(9) Peersen, O. B.; Wu, X.; Smith, S. O. *J. Magn. Reson., Ser. A* **1994**, *106*, 127–131.
(10) Bowmaker, G. A.; Dance, I. G.; Dobson, B. C.; Rogers, D. A. *Aust. J. Chem.* **1984**, *37*, 1607.
(11) Watton, S. P. Ph.D. Thesis. Northwestern University, Evanston, IL, 1993.
(12) Watton, S. P.; Bryson, J. W.; O'Halloran, T. V. Manuscript in preparation.
(13) Bryson, S. P.; Johnson, S. L.; Stern, C.; O'Halloran, T. V. Manuscript in preparation.

strengths in a range of 1−255 digital steps with a step size of approximately 1.2 kHz for ^{113}Cd and 1.5 kHz for ^{199}Hg.[14] For calibration of the B_1 field strength, 90° pulses were determined for the range of rf amplitudes used in the pulse sequence. The Hartmann−Hahn matching profiles were acquired in the same fashion as in Peersen et al. (1993).[7] Several sets of spectra were obtained by varying ω_{1X} from 25 to 83 kHz. For each set either one, five, nine, or eleven amplitudes were used on the proton channel during the CP contact time. The experiments with a single amplitude on the ^1H channel correspond to conventional cross polarization with a ω_{1H} spin-lock frequency of ~47 kHz. With five, nine, and eleven amplitudes, ω_{1H} was centered at 47 kHz and varied within frequency windows of 6.6, 11.8, and 18.6 kHz, respectively. The widow width is obtained from the difference between the largest and smallest proton spin-lock frequencies. The total contact time was kept constant at 10 ms and was equally divided among the multiple proton amplitudes in VACP. For example, the contact time of each individual amplitude was 1.1 ms when nine amplitudes were used. Only one isotropic resonance is present in the spectrum of each compound, but the signal intensity is distributed between the centerband and several rotational sidebands. The Hartmann−Hahn profiles were plotted as total signal intensity, summed over the entire spectrum, versus $\Delta\omega_1$. In the VACP experiment, $\Delta\omega_1$ is the difference between ω_{1X} and the *center* of the multiple ω_{1H} frequencies, set up to be ~47 kHz in this study, and corresponds to the first amplitude in the pulse sequence (Figure 1). The MAS speed was controlled to within 3 Hz with a spinning speed controller from Doty Scientific.

Results and Discussion

The two complexes $[Me_4N][Hg(S^iPr)_3]$ and $[Me_4N]_2[Cd_2(S^iPr)_6]$ were selected for this investigation for several reasons. Each complex serves as a model for a metalloprotein coordination environment of interest to the field of bioinorganic chemistry: $[Me_4N][Hg(S^iPr)_3]$ for the mercury metalloregulatory protein MerR[3] and $[Me_4N]_2[Cd_2(S^iPr)_6]$ for the family of zinc-binding regulatory proteins exemplified by the yeast transcriptional factor GAL.[15] X-ray crystal structures have been determined for both complexes.[12,13] $[Me_4N][Hg(S^iPr)_3]$ consists of discrete mononuclear $[Hg(S^iPr)_3]^-$ units with crystallographic trigonal symmetry.[12] $[Me_4N]_2[Cd_2(S^iPr)_6]$ consists of dimeric dianionic $[Cd_2(S^iPr)_6]^{2-}$ units in which each Cd(II) ion is bound by two terminal thiolate ligands and two bridging ligands in a distorted tetrahedral geometry.[13] Both complexes have fairly large CSAs and have a single proton per ligand available for efficient cross polarization. These two complexes thus present a fair yet challenging test of the benefits of the VACP technique.

The effect of high spinning speed on the CP-MAS spectra of $[Me_4N][Hg(S^iPr)_3]$ is shown in Figure 2 at ω_R = 4, 8, and 12 kHz using conventional single-amplitude cross polarization (SACP) at the exact Hartmann−Hahn matching condition ($\Delta\omega_1$ = 0 kHz). The NMR signal of the single ^{199}Hg resonance is dispersed over ~1250 ppm. The most intense peak in Figure 2 increases from 15% of the total intensity at 4 kHz to 41% at 12 kHz. Therefore, a corresponding increase in the signal-to-noise ratio of approximately 3-fold would be expected by increasing the MAS frequency from 4 to 12 kHz *if* the total intensity remains the same. However, the total intensity obtained in the conventional SACP experiment is not constant at the exact matching condition but *decreases* about 3-fold when ω_R increases from 4 to 12 kHz. As a result, the signal-to-noise ratio remains roughly constant in spite of the better averaging of the CSA. Similar results are observed for the $[Me_4N]_2[Cd_2(S^iPr)_6]$ complex (data not shown). This illustrates one of the major problems of combining conventional CP with high-speed MAS.

(14) The amplitude of the B_1 field is described in terms of the precession frequency $\omega_1 = \gamma B_1$.

(15) Marmorstein, R.; Carey, M.; Ptashne, M.; Harrison, S. C. *Nature* **1992**, *356*, 408−414.

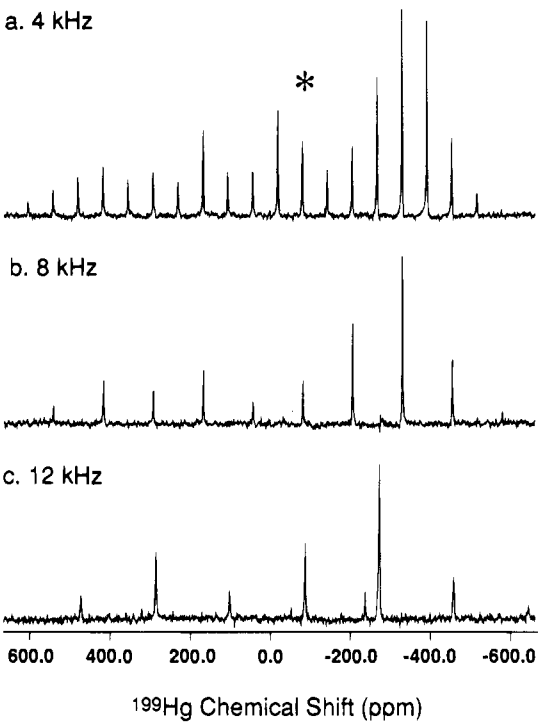

Figure 2. CP-MAS NMR spectra of $[Me_4N][Hg(S^iPr)_3]$ at spinning speeds of 4 (a), 8 (b), and 12 kHz (c). 1028 transients were collected with a 2.5 s acquisition delay and processed using line broadening of 100 Hz. Spectra were obtained at the exact Hartmann−Hahn matching condition and referenced to external $(CH_3)_2Hg$. The isotropic resonance at −79 ppm is marked with an asterisk. The additional peak in (c) is present in only some spectra and is presumably due to a second component in the sample.

The Hartmann−Hahn matching curves at 4 kHz MAS are shown in Figure 3a,d for $[Me_4N]_2[Cd_2(S^iPr)_6]$ and $[Me_4N][Hg(S^iPr)_3]$, respectively. The curves have fairly flat profiles that are 15−20 kHz wide, indicating that maximum signal is observed over a wide range of matching conditions ($\Delta\omega_1$). This broadening results from strong H−X dipolar couplings at low ω_R that can compensate for slight mismatches in the spin-lock field. The plateau is further broadened by several kilohertz using VACP with five and nine amplitudes. A weak oscillation can be observed in the profile of the $[Me_4N]_2[Cd_2(SiPr)_6]$ sample at 4 kHz MAS (Figure 3a) and appears in the $[Me_4N][Hg(S^iPr)_3]$ curves at ~5 kHz (data not shown). It is clear from these profiles that at low MAS speeds it is easy to locate and maintain an optimal matching condition using either the conventional SACP or VACP pulse sequences.

Drastic changes are observed in the SACP matching curves when the MAS frequency is increased to 8 kHz (Figure 3b,e, open circles). Instead of a flat profile, pronounced oscillations are observed that are regularly spaced by ω_R, greatly reducing the chance of residing at a local maximum. The total intensity is also lower compared to that obtained at ω_R = 4 kHz. VACP shows a marked improvement over SACP at ω_R = 8 kHz. The oscillation is substantially diminished when five amplitudes are used (Figure 3b,e, dotted lines), and the profile is completely flat using nine amplitudes (solid lines).

The benefit of using the VACP sequence is clearly illustrated in Figure 4, where the $[Me_4N]_2[Cd_2(S^iPr)_6]$ spectra obtained at different matching conditions ($\Delta\omega_1$) are plotted using SACP (a) and using VACP (b) with nine amplitudes. In the SACP case, large changes in signal intensity occur when $\Delta\omega_1$ differs by only a few kilohertz (Figure 4a). It is important to emphasize that, for systems with low sensitivity where it is not practical to acquire a Hartmann−Hahn profile, it can be difficult to locate

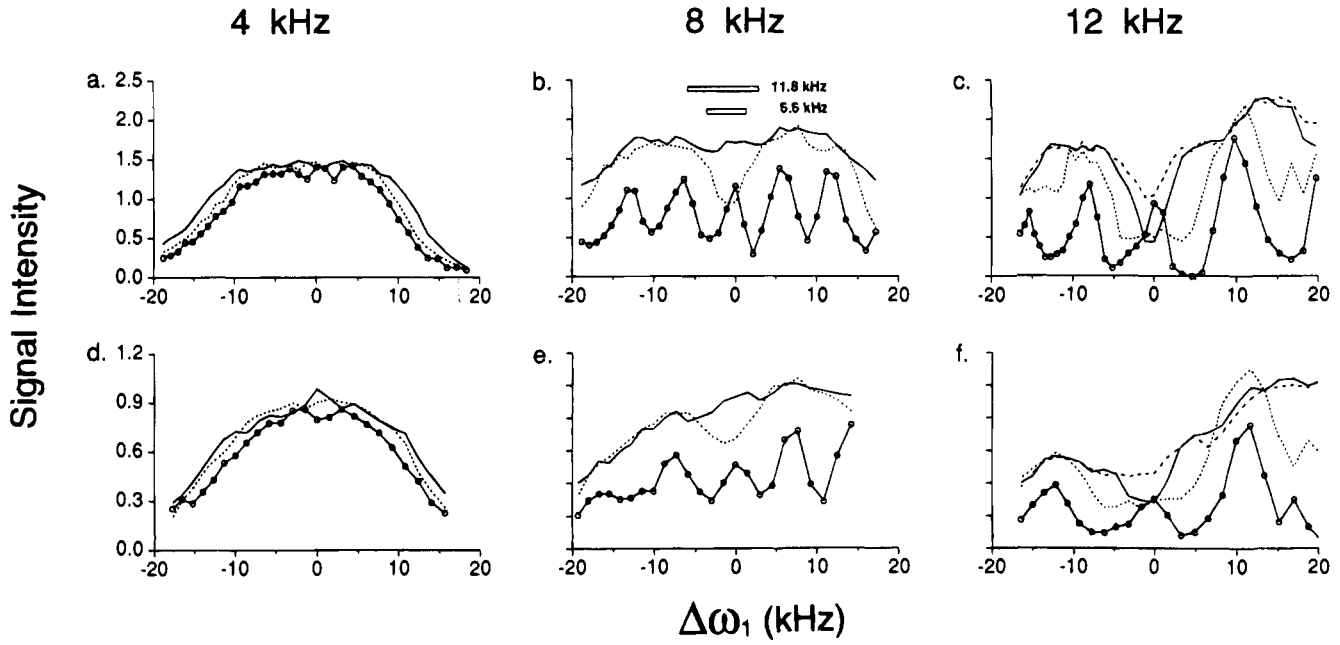

Figure 3. SACP and VACP Hartmann–Hahn matching curves for $[Me_4N]_2[Cd_2(S^iPr)_6]$ (top) and $[Me_4N][Hg(S^iPr)_3]$ (bottom) at MAS speeds of 4, 8, and 12 kHz. The individual data points (○) are shown for the SACP profiles but have been removed for clarity in the VACP curves using five (•••), nine (—), and eleven (- - -, Figure 3c,f only) amplitudes. The hollow bars in Figure 3b represent the proton window width for five and nine amplitudes, respectively, centered at $\Delta\omega_1 = 0$. The signal intensities are the sum of intensities of the center and spinning sidebands from the single isotropic resonance and are presented in arbitrary units and directly comparable at different MAS frequencies.

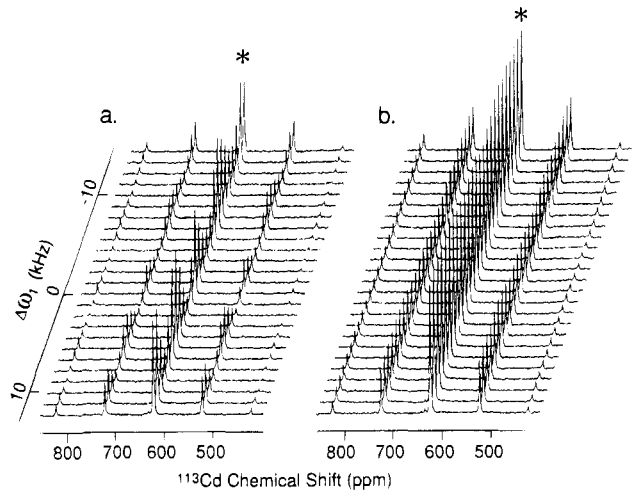

Figure 4. Comparison of $[Me_4N]_2[Cd_2(S^iPr)_6]$ spectra taken at ω_R = 8 kHz using SACP (a) and using VACP (b) with nine amplitudes at a series of Hartmann–Hahn matching conditions ($\Delta\omega_1$). The spectra are referenced to 0.1 M $Cd(ClO_4)$ in H_2O, and the 627 ppm isotropic peaks are labeled with an asterisk.

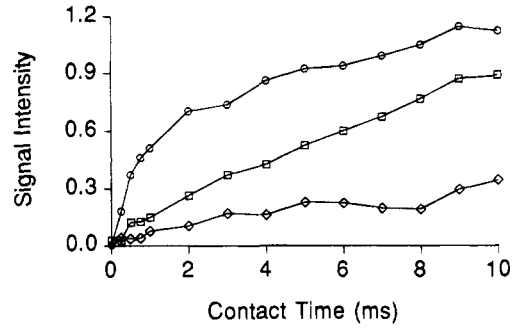

Figure 5. Cross polarization buildup curves of $[Me_4N]_2[Cd_2(S^iPr)_6]$ obtained at $\Delta\omega_1 = 0$ (□), $\Delta\omega_1 = \omega_R$ (○), and $\Delta\omega_1 = 0.5\omega_R$ (◇) in the 8 kHz Hartmann–Hahn profile illustrating the difference in buildup rates at different matching conditions.

the exact matching condition. In addition, even when the matching condition can be obtained, it is difficult to maintain it within a few kilohertz during data acquisition due to fluctuations in amplifier stability and probe tuning. The series of spectra obtained with VACP (Figure 4b) exhibit a substantial increase in intensity (~50%) compared to the maximum signal obtained using SACP, and more importantly, the observed signal is independent of the CP matching condition over a range of 25 kHz. Therefore, finding and maintaining an optimal matching condition is no longer a problem. Similar effects are observed at ω_R = 12 kHz (Figure 3c,f).

In order to optimize the data acquisition using VACP with the goal of obtaining a flat profile and recovering full intensity, there are several interdependent parameters that must be considered. These include the contact time, number of amplitudes, amplitude step size, and MAS speed. First, the total contact time required in the VACP experiment is lengthened relative to that of an optimized SACP experiment since only a few of the amplitudes in the VACP sequence yield maximum signal. An upper limit on the total contact time is often set by the amplifier specifications or the $T_{1\varrho}$ of the system. In the experiments discussed above, we used a constant total contact time of 10 ms due to an amplifier limitation. The $T_{1\varrho}$ values for Cd, Hg, and H in the two model compounds are relatively long (>10 ms) and are generally greater than the T_{HgH} and T_{CdH} time constants for cross polarization (e.g. see Figure 5). Under these conditions, the total contact time is not a limiting factor.[16] Second, the contact time for each individual amplitude has to be long enough so that sufficient CP buildup can occur at the optimal matching conditions. The buildup rates are compound-dependent and vary as a function of $\Delta\omega_1$. The fastest rates are observed at the matching sidebands ($\Delta\omega_1 = n\omega_R$, $n = \pm1$ and ±2)[6] where it takes about 1 ms to reach 50% of the maximum

(16) If the $T_{1\varrho}$ values are extremely short, then the VACP method does not work effectively since the total contact time exceeds $T_{1\varrho}$. Under these conditions, the optimal experimental setup is to use an increasing ramp of amplitudes on one of the matching sidebands of the Hartmann–Hahn profile, which allows one to shorten the total contact time. This is discussed more fully in ref 8.

signal for the cadmium compounds (Figure 5, open circles). The buildup curve for the trigonal mercury complex exhibits a similar rate (data not shown). The number of amplitudes is restricted by the limitation imposed on the total and individual contact times as discussed above. For the metal complexes, the use of ten amplitudes or less ensures that each amplitude lasts at least 1 ms under our 10 ms total contact time constraint. Third, the amplitude step size should be smaller than half of the width of a matching peak in the SACP profile. This ensures that at least two of the amplitudes correspond to matching conditions that generate better than 50% of the maximum signal in the SACP profile. In this study, the width of the matching peaks is about 5 kHz for both compounds (Figure 3) and an average step size of 1.3 kHz is used between proton amplitudes. Finally, the proton window width, determined by the product of the step size and the number of amplitudes, should be larger than ω_R so that one of the matching peaks is always sampled. For a well-characterized system, it is straightforward to make an appropriate choice of the total contact time, the number of amplitudes, and the amplitude step size at a given MAS speed. For an unknown system, the VACP parameters can be chosen on the basis of related compounds and an efficient matching condition can be readily located since VACP significantly broadens the matching profile. For example, this study provides the initial parameters for setting up VACP experiments of other cadmium and mercury complexes and metalloproteins.

There are several features of the Hartmann–Hahn profiles that warrant additional discussion. First, there is a drastic decrease in signal intensity at the exact matching condition using five amplitudes in the $\omega_R = 8$ kHz VACP curves (Figure 3b,e) and using five, nine, or eleven amplitudes in the 12 kHz curves (Figure 3c,f). This is because the cross polarization buildup rate at the matching centerband is much slower than that at the first and second sidebands, where $\Delta\omega_1 = \pm\omega_R$ and $\Delta\omega_1 = \pm 2\omega_R$, respectively (Figure 5).[6,17] When the proton window width spans only the $\Delta\omega_1 = 0$ matching peak, very little signal is generated. This can be overcome by increasing the window width so that one of the matching side peaks is covered, as shown in Figure 3b. The window width is 6.6 kHz using five amplitudes and is not wide enough to reach either the $+\omega_R$ or $-\omega_R$ matching sideband; therefore a valley is formed centered at $\Delta\omega_1 = 0$ (Figure 3b; see insert and dotted line). The window width increases to 11.8 kHz when nine amplitudes are used and is large enough to always cover at least one matching sideband. As a result, a flat profile with full intensity is obtained (Figure 3b; see insert and solid line). This becomes difficult to achieve at very high MAS speeds where wider window widths are obtained at the expense of sufficient contact time at the individual amplitudes due to the limited total contact time (Figure 3c, dashed line). In general, it is advisable to avoid the exact matching condition and to reside on a matching sideband. Fortunately, there is always a wide range of matching conditions (over 10 kHz) away from $\Delta\omega_1 = 0$ in the Hartmann–Hahn profiles that can be easily located and yield high intensity.

A second interesting observation is the gradual decrease of total signal intensity in the Hartmann–Hahn profile for the Hg complex with decreasing $\Delta\omega_1$. This is in contrast to the Cd complex that exhibits relative constant signal over $\Delta\omega_1$ (compare parts b and e of Figure 3). This phenomenon may be due to the large CSA of the Hg complex (70 kHz) relative to that of the Cd complex (35 kHz). A large CSA results in a substantial offset ($\Delta\nu$) from the carrier frequency for spins at certain orientations. If the carrier frequency is at the exact Hartmann–Hahn match, the mismatch ($\Delta\omega_{HHM}$) due to $\Delta\nu$ is given by

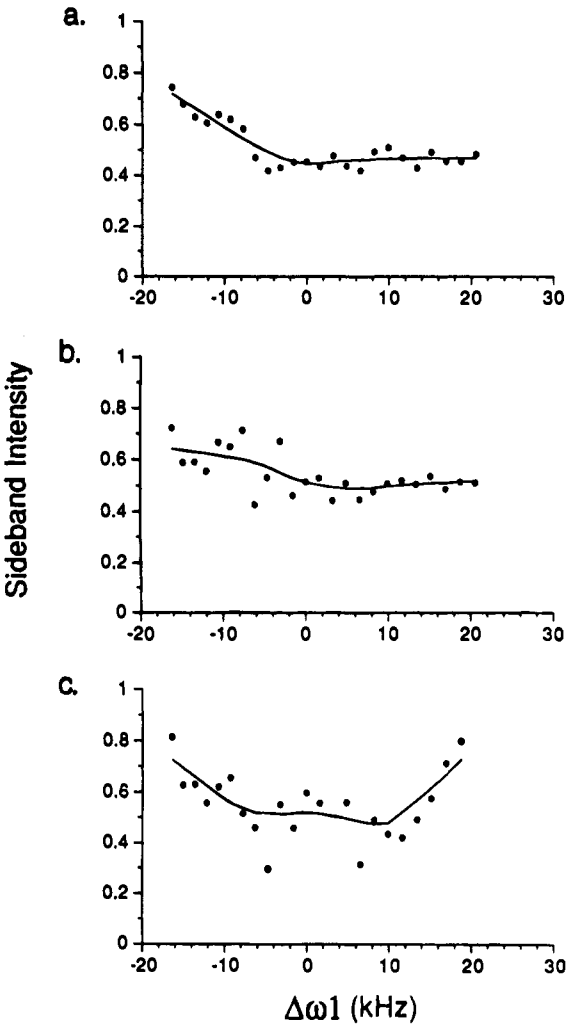

Figure 6. Normalized intensity of the +2 MAS sideband of $[Me_4N][Hg(S^iPr)_3]$ as function of $\Delta\omega_1$ using eleven amplitudes (a), five amplitudes (b), or one amplitude (c). The sideband intensity was normalized to the centerband intensity. The solid lines are the weighted fits to the data points. The MAS frequency was 12 kHz.

Artemov as follows:[18]

$$\Delta\omega_{HHM} = (\Delta\nu^2 + \omega_{1X}^2)^{1/2} - \omega_{1X}$$

For example, for the Hg complex, $\Delta\nu$ can be as large as 35 kHz. This corresponds to a $\Delta\omega_{HHM}$ of 11 kHz at $\omega_{1X} = 50$ kHz. The mismatch is even larger at lower ω_{1X} spin-lock frequencies. In contrast, the maximum mismatch is only 3 kHz for the cadmium compound due to the smaller CSA. Mismatching of certain spin orientations due to large CSAs has been shown to cause a decrease in the signal intensity[19] and is likely to be responsible for the observed difference in the Hg and Cd Hartmann–Hahn matching profiles. VACP can partially recover the signal by generating multiple matching conditions. For the Hg complex, however, full intensity cannot be achieved at lower ω_{1X} due to the extremely large CSA, and it is necessary to apply a higher spin-lock field to obtain maximum signal.

Since stable and accurate sideband intensities are essential for extracting the chemical shift tensor elements from the MAS spectrum, the effect of Hartmann–Hahn mismatches must be taken into account. Besides a decrease in signal intensity, another consequence of the Hartmann–Hahn mismatch de-

(17) Wu, X.; Zilm, K. W. *J. Magn. Reson., Ser. A* **1993**, *102*, 205–213.

(18) Artemov, D. Yu. *J. Magn. Reson.* **1991**, *91*, 405–407.

(19) Jeschke, G.; Grossmann, G. *J. Magn. Reson., Ser. A* **1993**, *103*, 323–328.

scribed above is that the sideband intensities are likely to be distorted at high MAS speeds for compounds with large CSAs. This is illustrated in Figure 6, which plots the intensity of the +2 sideband (relative to the intensity of the centerband) in the 12 kHz MAS spectrum of the Hg complex as a function of $\Delta\omega_1$. With eleven amplitudes (Figure 6a), the normalized intensity is stable at high values of $\Delta\omega_1$ (high Hg B_1 field strengths) and corresponds to the intensity obtained in a single-pulse Bloch decay experiment (data not shown). As $\Delta\omega_1$ is reduced, the intensity becomes dependent on the B_1 field strength. With five amplitudes (Figure 6b), the B_1 field dependence occurs at higher field strengths and stable intensities are only observed above $\Delta\omega_1 \sim 10$ kHz. Finally, with one amplitude (Figure 6c), there is a large scatter in the normalized intensity over the range of $\Delta\omega_1$ values. Similar plots are observed for the other sidebands in the MAS spectrum and at lower spinning speeds as long as the Hartmann–Hahn profile exhibits oscillations. Combined with the conclusions from the previous two paragraphs, these observations indicate that for ^{199}Hg CP-MAS NMR it is best to center the matching condition in the vicinity of the $+\omega_R$ matching sideband, where VACP gives maximum and stable intensity over a 10 kHz range of matching conditions.

An important consequence of the above observations is that, for systems that have more than one resonance, a mismatch due to a difference in chemical shift may cause a displacement of the Hartmann–Hahn matching profile along $\Delta\omega_1$ at high ω_R. As a result, for systems with large chemical shift ranges, such as metal complexes, it may not be possible to reside at the optimal matching condition for several resonances simultaneously using conventional SACP. The VACP sequence can overcome this problem by including the optimal matching condition required for each resonance.

A third notable feature of the VACP Hartmann–Hahn profiles is the increase of total intensity relative to conventional SACP at higher ω_R (Figure 3b,c,e,f). This is attributed to the ability of VACP to compensate for the loss of intensity at the matching peaks of the SACP profiles due to the effects of inhomogeneous B_1 fields. A detailed discussion of this effect for adamantane can be found in Peersen et al. (1993).[9] Briefly, the B_1 field generated by a CP pulse is not constant throughout the single-solenoid sample coils generally used in MAS probes; the B_1 field is much lower at the ends of the coil than at the center. This presents a problem when a full rotor is used and the sample extends beyond the region of a homogeneous B_1 field in the center of the coil, which is usually the situation for most applications. The loss of signal intensity results from the fact that there is not an exact match between ω_R and $\Delta\omega_1$ at a matching sideband *throughout the sample* because $\Delta\omega_1$ will vary depending on the position in the coil. In other words, only part of the sample at the center of the coil is exactly matched and gives rise to significant signal. VACP compensates for this mismatch at the ends of the coil by providing multiple matching conditions and therefore restores full intensity.

In summary, the weak heteronuclear dipolar interactions and large CSAs of metal complexes present problems for conventional CP-MAS NMR. The high MAS frequencies required for averaging the CSA lead to oscillations in the Hartmann–Hahn matching curves, a situation shared by many systems. VACP is shown to be extremely useful in such cases. It allows the gain in signal-to-noise at higher spinning speeds to be fully expressed by generating flat Hartmann–Hahn matching curves with high intensity. These results extend the previous work on ^{13}C[7-9] and show that VACP can be generally applied to any system where conventional CP is effective. It is especially valuable for systems that have low intrinsic sensitivity, such as proteins, where optimal matching conditions must be located without extensive searching.

Acknowledgment. The authors thank Dr. Günther Metz and Dr. Xiaoling Wu for helpful discussions.

IC940723H